Electron spin resonance on a 2D van der Waals $CrBr_3$ uniaxial ferromagnet

G. Clemente,[1] M. Moret, [1] A. Granados del Águila,[2] M. Hussain,[3] Z. Sofer,[3] X. Liu,[4] M. Fanciulli,[1] and F. Moro[1, a)]

AFFILIATIONS

[1] Department of Materials Science, University of Milano-Bicocca, via R. Cozzi 55, Milano 20125, Italy.

[2] Institute for Functional Intelligent Materials, National University of Singapore, 117544, Singapore.

[3] Department of Inorganic Chemistry, Faculty of Chemical Technology, University of Chemistry and Technology Prague, Technicka 5, 16628 6 Prague, Czech Republic

[4] Information Materials and Intelligent Sensing Laboratory of Anhui Province, Institutes of Physical Science and Information Technology, Anhui University, Hefei 230601, China.

[a)] **Author to whom correspondence should be addressed:** Fabrizio.moro@unimib.it

Keywords: $CrBr_3$; 2D magnets; electron spin resonance; uniaxial anisotropy

ABSTRACT

We report on the electron spin resonance properties (ESR) of a van der Waals bulk $CrBr_3$ single crystal. Angular and temperature dependent studies are performed in the range of the critical temperature for ferromagnetic order. The angular dependent data enable the determination of a strong uniaxial magnetic anisotropy constant, *K* with the easy axis of the magentization being paralellel to the crystallographic *c* axis. The peak-to-peak ESR linewidth below the Curie – temperature shows contributions from the term $(3\cos^2\theta - 1)^2$, thus suggesting the occurance of long-wavelength ($q \rightarrow 0$) modes of spin fluctuations typical for 2D systems. Finally we analyse the temperature dependence of the double integrated ESR intensity, resonance field and

linewidth for the direction of the magnetic field parallel and perpendicular to the *c* easy axis. We determine the Weiss's contants, the thermal dependence of *K* and observe the crossover region from linewidth narrowing to broadening approaching the critical temperature. Overall, our findings show that bulk $CrBr_3$ single crystals behave like a 2D ferromagnet with uniaxial anisotropy.

I. INTRODUCTION

Van der Waals magnets are gaining interest because they can be exploited for making new devices in spintronics and optoelectronics.[1-6] They are also interesting materials from the fundamental point of view because new quantum phenomena and topological phase transitions can be observed.[7-11] Among the large family of 2D magnets, the series of chromium trihalides CrX_3 (X = Cl, Br and I) is one of the most investigated.[12]

There is a long standing interest around Cr-based trihalides. For instance $CrBr_3$ was the first ferromagnetic semiconductor found by Tsubokawa in 1960[13] whereas CrI_3 was one of the first materials studied by ESR.[12] Magnetic properties of the Cr-based trihalides have been reported by conventional magnetometer[3,13], electron spin resonance[12,14-18], Raman spectroscopy[19-23] as well as theoretically predicted.[24-26]

Their magnetic properties arise from the octahedrally coordinated Cr ions in the oxidation state +3 which leads to a spin S = 3/2 according to the Hund's rule and quenched orbital magnetic moment. These octahedra form edge-sharing networks in the crystallographic *ab* plane resulting in a magnetic honeycomb lattice which interacts by van der Waals interactions along the *c* axis and are spaced by ~ 0.7 nm (**Figure 1**).

Although Cr-based trihalides are structurally similar, surprisingly, they have rather different magnetic properties. $CrBr_3$ and CrI_3 show ferromagnetic interlayer coupling with Curie transition temperatures T_C = 32.5 K and 16.8 K respectively, whereas $CrCl_3$ shows a antiferromagnetic interlayer coupling with Néel temperature T_N = 68 K.[14] In addition, $CrCl_3$ is an 2D-XY system with in plane easy axis of the magnetization,[27] whereas for $CrBr_3$ and CrI_3 the magnetization favours an alignment perpendicular to the Van der Waals layers.[28]

More recently, these materials have gained renewed interest within the research field of two dimensional materials because of their layer-dependent properties which makes them ideal as magnetic components within 2D heterostructure-based devices.[3,29,30] For instance intrinsic

ferromagnetism has been reported in a monolayer of CrI_3.[3] Moreover, interesting phenomena such as chiral phonons and giant magneto optical effects[31], van der Waals stacking–dependent interlayer magnetism,[32] magnon-assisted tunnelling [33] as well as light induced electron spin resonance properties in $CrCl_3$ and CrI_3[34] have been observed. Among these Cr-trihalides 2D magnets, $CrBr_3$ is particularly appealing from the technological point of view because of its stability to air, [3,35] robust 2D ferromagnetism and strong out of plane magnetic anisotropy.[36] In addition, heterostructure devices made by combining $CrBr_3$ with other 2D materials such as transition metal dichalcogenides[37,38] as well as SiC[39], GeC[40] graphene[41] are currently under investigation. Notwithstanding, only a few ESR studies have reported so far[16,17,42] and the understanding of magnetic anisotropy and spin model system in $CrBr_3$ is still under investigation.[36,43]

Here we report a comprehensive angular and temperature dependent ESR investigation of a bulk $CrBr_3$ single crystal which enable the determination of the easy axis of the magnetization, the magnetic anisotropy constant, *K*, and symmetry, and to get insights on the spin-spin correlations and spin dimensionality.

II. EXPERIMENTAL DETAILS

Single crystals of $CrBr_3$ were grown by the chemical vapor transport method and were mounted on a suprasil quartz rod and into a goniometer with ½ degree sensitivity for crystal rotation measurements. A flat crystal with surface size 2 x 3 mm^2 and thickness < 1 mm was selected to avoid saturation and distortion of the ESR signal. The ESR spectra were recorded with a Varian E15 spectrometer coupled to a Bruker super high Q cavity operated at X-band (~ 9.4 GHz). The static magnetic field was modulated at 100 kHz with modulation amplitude of 4 Gauss. The magnetic field was monitored continuously with an electronic counter and a Hall probe. Sample temperatures in the range 4–300 K were obtained with an Oxford ESR 900 cryostat. A DPPH sample was used as reference to determine the *g*-factors. MatLab generated routines were used to fit the spectra. Peak-to-peak linewidths ΔH were calculated from the full-width half maximum $\Delta H_{1/2}$ obtained from the Lorentzian fit with the relation: $\Delta H = \Delta H_{1/2}/\sqrt{3}$.

III. RESULTS

A. ESR angular dependence

The angular dependent electron spin resonance spectra for a $CrBr_3$ single crystal at T = 30 K and 55 K are reported in **Figure 2**. The crystal is rotated in the out-of-plane configuration, that is by rotating the crystal around crystallographic axis a with respect to the applied magnetic field H with rotation angle θ_H (**Figure 1c**). The spectra show a Lorentzian profile from where the magnetic resonance field, H_r and peak-to-peak linewidth, ΔH as function of θ_H are obtained and reported in **Figure 3**.

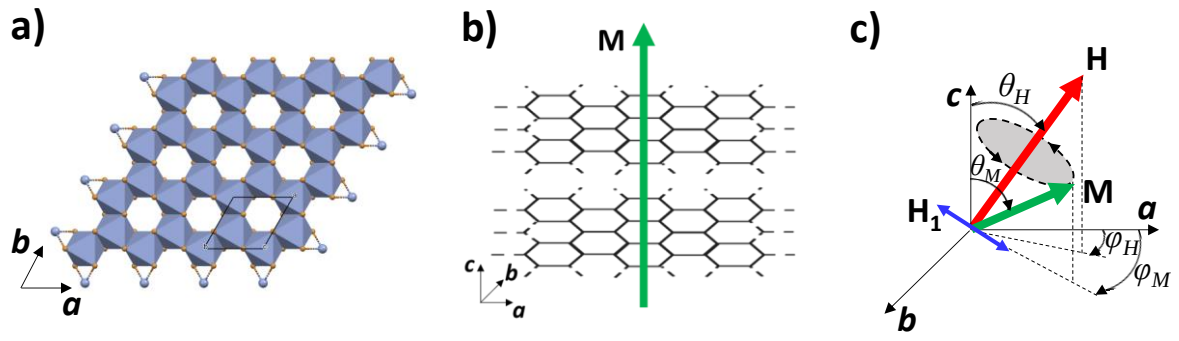

Figure 1. View of a single layer of the $CrBr_3$ crystal structure along the c axis. The octahedra sharing two corners are indicated along with the a and b axes of the P3 unit cell. Color code: Br – orange and Cr – blue. **b)** Perpendicular uniaxial anisotropy in $CrBr_3$. **c**) Representation of the configuration used for the angular dependent studies with rotation angles θ_H formed between the magnetic field direction H and the c axis. Precession of the magnetization vector M (green vector) around the magnetic field H (red vector) perpendicular to the microwave field H_1 (blue double arrowed line) in the ESR experiment. The magnetization absorbs the microwave energy when the precession frequency matches the frequency of the microwave photons.

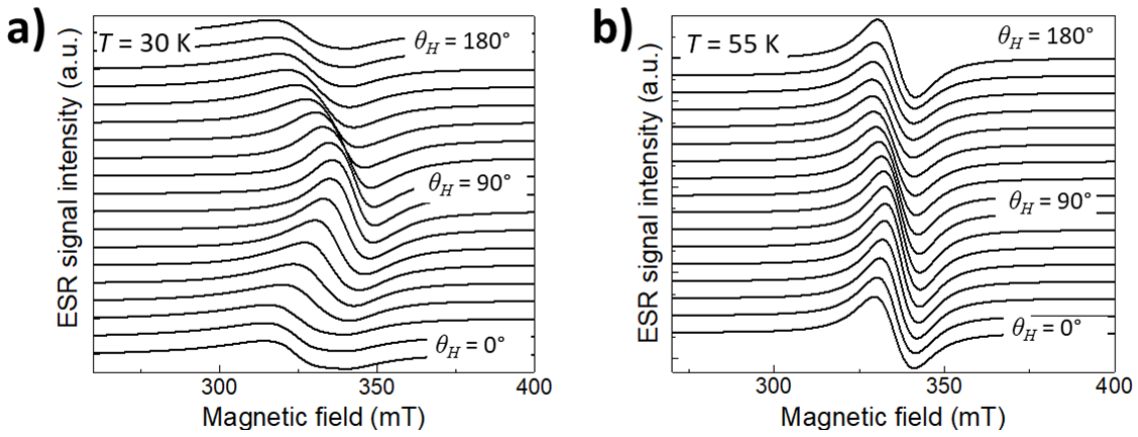

Figure 2 Angular dependent electron spin resonance spectra recorded at temperature T = 30 K which is close to T_c (**a**) and for T = 55 K (**b**).

For T = 30 K, the magnetic resonance field H_r shows an axial-like symmetry with maxima and minima close to the crystallographic directions *b* and *c*, respectively. The data can be fitted to the equation:

$$H_r(\theta_H) = H_i cos^2(\theta_H) + H_0 \quad (1)$$

where H_i is the perpendicular internal anisotropy fields and H_0 is a magnetic field offset. From the result of the fit we obtain H_i (30 K) = (55 ± 1) mT. For T = 55 K, the spectra show a weak dependence with θ_H, and the fitting to the **Equation 1** provides H_i (55K) = (9.4 ± 0.2) mT.

The angular dependence of the peak-to-peak ESR linewidth, ΔH for T = 30 and 55 K (**Figure 3**) shows in both cases a periodic evolution with maxima and minima centered around the axes *c* and *b*, respectively. We note that for T = 30 K, ΔH shows a broader minimum with respect to T = 55 K. We fit the data by using the following general expression:[15]

$$\Delta H(\theta_H) = \mathrm{A}(3\cos^2(\theta_H) - 1)^2 + \mathrm{B}cos^2(\theta_H) + \Delta H_0 \quad (2)$$

where the linewidth amplitude constants are: A = 5.6 mT (0.75 mT) and B = 83.7 mT (15.5 mT) and the offset ΔH_0 = 127.8 mT (102 mT) for T = 30 K (55 K).

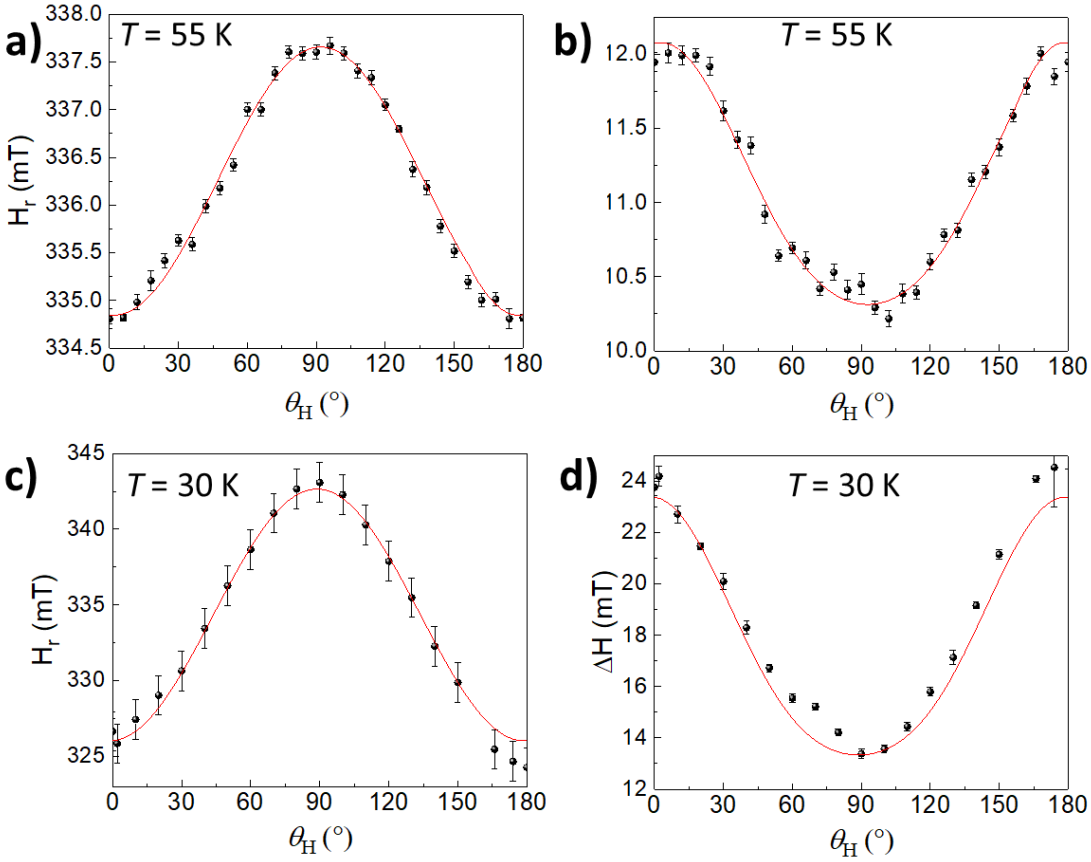

Figure 3 Angular dependence of the magnetic resonance field (**a** and **c**) and peak-to-peak linewidth (**b** and **d**) obtained from the Lorentzian fitting of the spectra in **Figure 2** at T = 30 K and 55 K. Circles and solid lines are the experimental data and simulations respectively (see text).

B. ESR temperature dependence

Temperature dependent spectra recorded for $H \perp c$ and $H \parallel c$ are reported in **Figure 4**. In both cases the spectra show a Lorentzian lineshape from room temperature down to 30 K with a gradual increase of intensity. For T < 30 K the spectra evolve into multiple resonances across the whole magnetic field range investigated with an overall decrease of the signal which tent to vanish down to T = 5 K (not shown). For T < 150 K and $H \perp c$ we observe that the spectra shift to higher fields with a small degree of broadening, whereas for $H \parallel c$ the spectra shift to lower fields with a significant linewidth broadening.

In **Figure 5a** the temperature dependence of the reciprocal of the double integrated area of the ESR signal proportional to the imaginary component of the magnetic susceptibility (χ) is shown. For H // c and $H \perp c$, χ^{-1} follows a linear dependence for T > 100 K while at lower temperatures it plateaus to zero. By fitting the data in the temperature region with linear dependence to the Curie-Weiss's law $\chi^{-1} = C/(T + \theta_W)$, where C is the Curie constant and θ_W the Weiss constant, we obtain $\theta_W^{\perp} \sim +$ (72 ± 8) K and $\theta_W^{\parallel} = +$ (89 ± 20) K for the H // c and $H \perp c$, respectively.

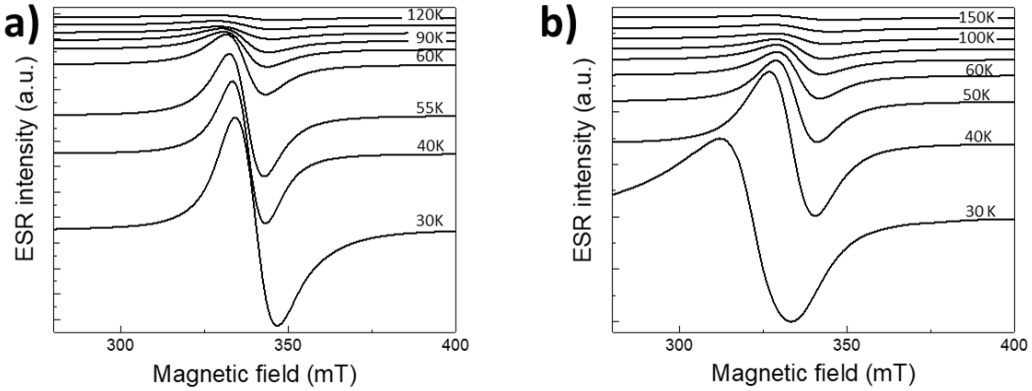

Figure 4 Temperature dependence of the electron spin resonance spectra recorded for $H \perp c$ (**a**) and H // c (**b**).

The temperature dependence of H_r for H // c and $H \perp c$ (hereafter $H_r^{\perp}$ and $H_r^{\parallel}$) are reported in **Figure 5b**. At room temperature, $H_r^{\perp} = H_r^{\parallel}$ = 336.8 mT (g-value = 2.008) and they both depend on the temperature by only ~ 1 % for T > 150 K. At lower temperatures $H_r^{\perp}$ and $H_r^{\parallel}$ increases and decreases respectively in a non-linear fashion. Below 50 K, $H_r^{\perp}$ and $H_r^{\parallel}$ increases and decreases respectively by approaching the Curie temperature, $T_C \sim$ 30 K. The temperature dependence of ΔH for H // c and $H \perp c$ (hereafter $\Delta H^{\perp}$ and $\Delta H^{\parallel}$) are shown in **Figure 5c**. At room temperature**,** $\Delta H^{\perp}$ = 269.7 mT and $\Delta H^{\parallel}$ = 266.6 mT. Upon cooling both $\Delta H^{\perp}$ and $\Delta H^{\parallel}$ decrease gradually in nearly linear fashion, reaching a minimum around 50 K. For T < 30 K the spectra evolve into a multi resonance spectra which makes the analysis of the resonance field and linewidth cumbersome.

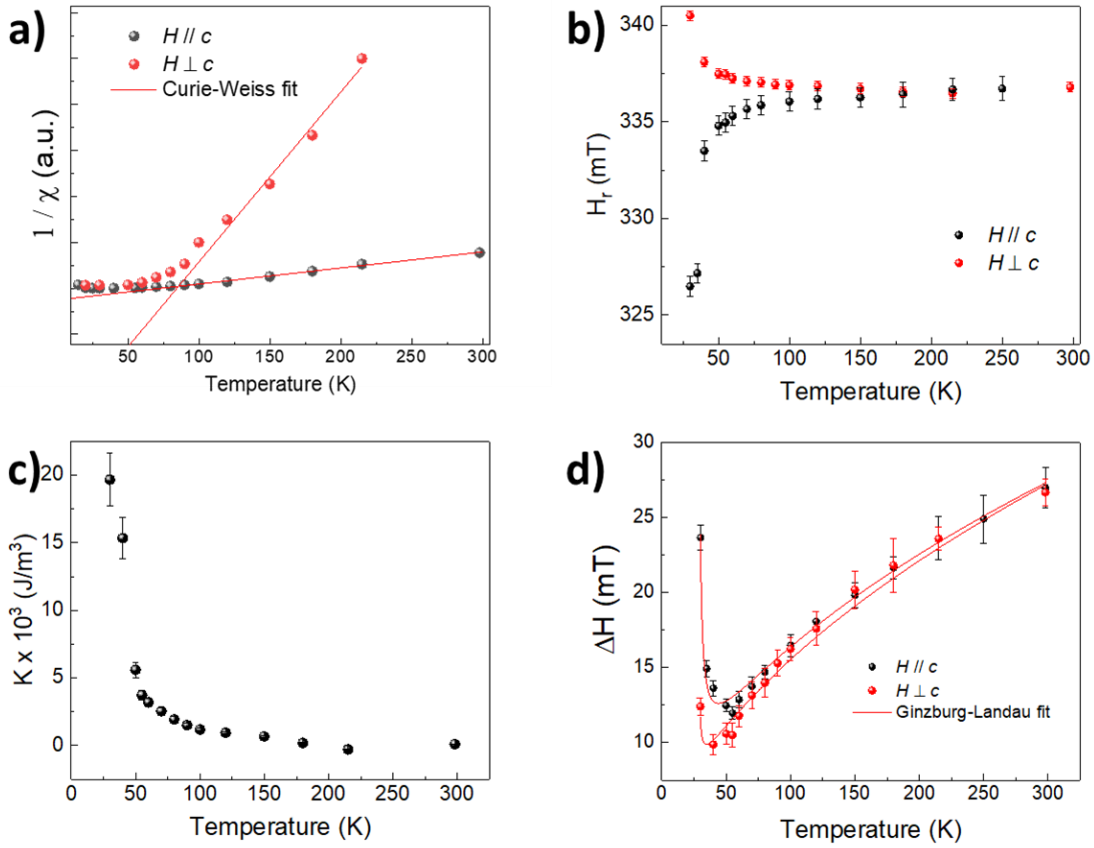

Figure 5 Temperature dependence of χ^{-1} (**a**), H_r (**b**), K (**c**) and ΔH (**d**). Lines in (**a**) are fit to the Curie-Weiss law (see text). Continuous red curves in **d**) are fitting according to the Ginzburg-Landau model (**Equation 3**).

IV. DISCUSSION

The angular dependent ESR studies performed at a temperature close to the Curie temperature T_C (*i.e.* T = 30 K) and above it (*i.e.* T = 55 K) reveal the direction of the magnetization axes as well as the strength of the magnetic anisotropy and symmetry. In particular, the sine-like dependence of the resonance field with the rotation angle θ_H indicates uniaxial magnetic anisotropy (**Figure 1b**). When the direction of the magnetic field is parallel to the easy and hard axes, the resonance field reaches the minimum and maximum values respectively.[44] Therefore, from the results in **Figure 3** we assign the easy axis of the magnetization to the *c* direction and the hard axis to the perpendicular direction.[16] The value of H_i obtained at T = 30 K is about 6 times larger than that

obtained at 55 K and reveal the temperature dependence of the magnetic anisotropy energy. From the relation: $K(T) = \Delta H_r(T)\, M_s / 2$, where $\Delta H_r = H_r^{\perp} - H_r^{\parallel}$, M_s if the saturation of the magnetization we estimate the anisotropy constant and its temperature dependence (**Figure 5c**) which increase from $K \sim 1$ KJ /m^3 for $T >$ 50 K to $K \sim 20$ KJ /m^3 for $T = 30$ K .[42]
The first and second terms in **Equation 2** correspond to the empirical dependence of the linewidth observed for 2D and 3D systems weighted by the factors A and B respectively. By comparing A / B at $T = 30$ K and 55 K, we obtain an increase of the 2D contribution at 30 K by about 40 %. Thus, these outcomes point towards the observations of 2D correlations in a ferromagnetic $CrBr_3$ single crystal[16] resulting from the dominant contribution of the long wavelength modes at $q \sim 0$.[15] The 2D correlation together with the out of plane easy axis of the magnetization (**Figure 1b**) are usually described by a simple Ising model. However, recent magnetic studies on few layer and monolayer have shown that CrB_3 behaves like a XXZ magnet instead of a simple Ising 2D magnet.[36] In addition, combined ESR and magnetic susceptibility studies of $CrBr_3$ have ruled out XY-like magnetism and the occurrence of a Berezinsky – Kosterlitz – Thouless (BKT) transition.[16]

The analysis of the temperature dependence of the double integrated ESR intensity in **Figure 5a** gives Weiss constants which are higher than the expected Curie temperature T_C ~30 K.[24,45] The discrepancy between the Weiss constants and T_C is ascribed to the effect of the applied magnetic field (~ 0.3 T) in the ESR experiment to lift the magnetic phase transition,[46] to magnetic frustration[47] or both.

The g-value = 2.008 at room temperature is close to the free electron g-value which indicates that the orbital moment of Cr^{3+} is quenched. Therefore, the contribution of the magnetocrystalline anisotropy is expected to be small. The opposite temperature dependences of the resonance field observed for $H \perp c$ and $H \,//\, c$ are consistent with the angular dependent studies and support the assignment of the magnetization axes.

Finally, we discuss the temperature dependence of the linewidth. It is worth noting that the ESR linewidth for $CrBr_3$ has been already reported at 9 GHz,[17] 24 GHz[17] as well as high ESR frequency (240 GHz).[16] The comparison between these studies have highlighted the effect of the ESR linewidth broadening for increased magnetic fields near the critical temperature T_C due to

magnetic field induced suppression of spin-spin correlation. In the regime of small magnetic fields such as that the $H << H_{exc}$, where H_{exc} is the exchange magnetic field, the linewidth is expected to increase for ferromagnets. However, the crossover from narrowing to broadening by approaching the critical temperature is rarely observed in ferromagnets and it has been reported to be suppressed for $CrBr_3$. More specifically, ERS studies of $CrBr_3$ at microwave frequencies 9 GHz and 24 GHz have reported a crossover region around 50 K with a weak maximum of ~10 mT for $H \parallel c$ whereas no crossover region was reported for $H \perp c$.[17,42] Instead, our findings show that the crossover of the linewidth near the critical temperature can be observed for both orientations $H \parallel c$ and $H \perp c$, and increases with no sign of suppression up to ~ 25 mT and ~ 12 mT respectively in agreement with theory.[48]

Finally, we analyse the temperature dependence of the linewidth with the Ginzburg-Landau critical model for the ESR linewidth:

$$\Delta H(T) = \frac{Q}{\left(\frac{T}{Tc} - 1\right)^{p}} + mT^{\alpha} + \Delta H \qquad (3)$$

where Q is a constant and p is the critical exponent depending mainly on type and sign of the interaction and on the dimension and symmetry of the spin lattice considered.[49] The second and third terms take into account the temperature dependence above T_C. From the fitting we obtain $p = 0.80 \pm 0.04$, $T_C = 29 \pm 1$ K and $\alpha = 0.5$ for both orientations. The value obtained for p is close to the one reported previously for other layered antiferromagnetic materials,[49] more specifically to the value reported for the same material system albeit at higher ESR frequency.[16]

V. CONCLUSIONS

In conclusion we have studied the magnetic properties of a bulk $CrBr_3$ single crystal. By exploiting the high sensitivity of the ESR technique we have obtained information about the fundamental magnetic properties such as magnetic anisotropy easy axis, magnetic anisotropy constant and symmetry as well as about spin-spin correlation and spin dimensionality with the critical phase transition parameter. In addition, we have observed the crossover temperature dependence of the ESR linewidth with diverging broadening near the Curie temperature in

agreement with the theory of ferromagnetic resonance. Overall, our findings show that $CrBr_3$ single crystal behaves like a 2D ferromagnet with strong uniaxial symmetry.

ACKNOWLEDGEMENTS

Z.S. was supported by project LTAUSA19034 from Ministry of Education Youth and Sports (MEYS).

REFERENCES

1 C. Gong, L. Li, Z. Li, H. Ji, A. Stern, Y. Xia, T. Cao, W. Bao, C. Wang, Y. Wang, Z. Q. Qiu, R. J. Cava, S. G. Louie, J. Xia, and X. Zhang, Nature **546,** 265 (2017).

2 J.-G. Park, Journal of Physics: Condensed Matter **28,** 301001 (2016).

3 B. Huang, G. Clark, E. Navarro-Moratalla, D. R. Klein, R. Cheng, K. L. Seyler, D. Zhong, E. Schmidgall, M. A. McGuire, D. H. Cobden, W. Yao, D. Xiao, P. Jarillo-Herrero, and X. D. Xu, Nature **546,** 270 (2017).

4 M. Gibertini, M. Koperski, A. F. Morpurgo, and K. S. Novoselov, Nature Nanotechnology **14,** 408 (2019).

5 K. S. Burch, D. Mandrus, and J. G. Park, Nature **563,** 47 (2018).

6 X. Jiang, Q. X. Liu, J. P. Xing, N. S. Liu, Y. Guo, Z. F. Liu, and J. J. Zhao, Applied Physics Reviews **8** (2021).

7 A. Ashoka, K. S. Bhagyashree, and S. V. Bhat, Physical Review B **102,** 024429 (2020).

8 J. Li, Y. Li, S. Du, Z. Wang, B.-L. Gu, S.-C. Zhang, K. He, W. Duan, and Y. Xu, Science Advances **5,** eaaw5685 (2019).

9 S. Kezilebieke, M. N. Huda, V. Vaňo, M. Aapro, S. C. Ganguli, O. J. Silveira, S. Głodzik, A. S. Foster, T. Ojanen, and P. Liljeroth, Nature **588,** 424 (2020).

10 H. Yang, S. W. Kim, M. Chhowalla, and Y. H. Lee, Nature Physics **13,** 931 (2017).

11 Z. W. Cai, S. Bao, Z. L. Gu, Y. P. Gao, Z. Ma, Y. Shangguan, W. D. Si, Z. Y. Dong, W. Wang, Y. Z. Wu, D. J. Lin, J. H. Wang, K. J. Ran, S. C. Li, D. Adroja, X. X. Xi, S. L. Yu, X. S. Wu, J. X. Li, and J. S. Wen, Physical Review B **104** (2021).

12 J. Zeisner, K. Mehlawat, A. Alfonsov, M. Roslova, T. Doert, A. Isaeva, B. Buchner, and V. Kataev, Physical Review Materials **4** (2020).

13 I. Tsubokawa, Journal of the Physical Society of Japan **15,** 1664 (1960).

14 R. W. Bené, Physical Review **178,** 497 (1969).

15 S. Chehab, J. Amiell, P. Biensan, and S. Flandrois, Physica B **173,** 211 (1991).

16 C. L. Saiz, J. A. Delgado, J. van Tol, T. Tartaglia, F. Tafti, and S. R. Singamaneni, Journal of Applied Physics **129** (2021).

17 M. S. Seehra and R. P. Gupta, Physical Review B **9,** 197 (1974).

18 X. Shen, H. Chen, Y. Li, H. Xia, F. Zeng, J. Xu, H. Y. Kwon, Y. Ji, C. Won, W. Zhang, and Y. Wu, Journal of Magnetism and Magnetic Materials **528,** 167772 (2021).

19 D. P. Kozlenko, O. N. Lis, S. E. Kichanov, E. V. Lukin, N. M. Belozerova, and B. N. Savenko, npj Quantum Materials **6,** 19 (2021).

20 W. C. Jin, Z. P. Ye, X. P. Luo, B. W. Yang, G. H. Ye, F. Z. Yin, H. H. Kim, L. Rojas, S. J. Tian, Y. Fu, S. H. Yan, H. C. Lei, K. Sun, A. W. Tsen, R. He, and L. Y. Zhao, Proceedings of the National Academy of Sciences of the United States of America **117,** 24664 (2020).

[21] A. McCreary, T. T. Mai, F. G. Utermohlen, J. R. Simpson, K. F. Garrity, X. Z. Feng, D. Shcherbakov, Y. L. Zhu, J. Hu, D. Weber, K. Watanabe, T. Taniguchi, J. E. Goldberger, Z. Q. Mao, C. N. Lau, Y. M. Lu, N. Trivedi, R. V. Aguilar, and A. R. H. Walker, Nature Communications **11** (2020).
[22] L. Webster, L. B. Liang, and J. A. Yan, Physical Chemistry Chemical Physics **20,** 23546 (2018).
[23] Y. J. Zhang, X. H. Wu, B. B. Lyu, M. H. Wu, S. X. Zhao, J. Y. Chen, M. Y. Jia, C. S. Zhang, L. Wang, X. W. Wang, Y. Z. Chen, J. W. Mei, T. Taniguchi, K. Watanabe, H. G. Yan, Q. H. Liu, L. Huang, Y. Zhao, and M. Y. Huang, Nano Letters **20,** 729 (2020).
[24] H. Wang, V. Eyert, and U. Schwingenschlögl, Journal of Physics: Condensed Matter **23,** 116003 (2011).
[25] D. Soriano, M. I. Katsnelson, and J. Fernández-Rossier, Nano Letters **20,** 6225 (2020).
[26] S. Tiwari, M. L. Van de Put, B. Sorée, and W. G. Vandenberghe, Physical Review B **103,** 014432 (2021).
[27] A. Bedoya-Pinto, J. R. Ji, A. K. Pandeya, P. Gargiani, M. Valvidares, P. Sessi, J. M. Taylor, F. Radu, K. Chang, and S. S. P. Parkin, Science **374,** 616 (2021).
[28] M. A. McGuire, G. Clark, K. C. Santosh, W. M. Chance, G. E. Jellison, V. R. Cooper, X. D. Xu, and B. C. Sales, Physical Review Materials **1** (2017).
[29] M. J. Hamer, D. G. Hopkinson, N. Clark, M. W. Zhou, W. D. Wang, Y. C. Zou, D. J. Kelly, T. H. Bointon, S. J. Haigh, and R. V. Gorbachev, Nano Letters **20,** 6582 (2020).
[30] L. Webster and J.-A. Yan, Physical Review B **98,** 144411 (2018).
[31] T. T. Yin, K. A. Ulman, S. Liu, A. G. del Aguila, Y. Q. Huang, L. F. Zhang, M. Serra, D. Sedmidubsky, Z. Sofer, S. Y. Quek, and Q. H. Xiong, Advanced Materials **33** (2021).
[32] W. O. Chen, Z. Y. Sun, Z. J. Wang, L. H. Gu, X. D. Xu, S. W. Wu, and C. L. Gao, Science **366,** 983 (2019).
[33] D. Ghazaryan, M. T. Greenaway, Z. Wang, V. H. Guarochico-Moreira, I. J. Vera-Marun, J. Yin, Y. Liao, S. V. Morozov, O. Kristanovski, A. I. Lichtenstein, M. I. Katsnelson, F. Withers, A. Mishchenko, L. Eaves, A. K. Geim, K. S. Novoselov, and A. Misra, Nature Electronics **1,** 344 (2018).
[34] S. R. Singamaneni, L. M. Martinez, J. Niklas, O. G. Poluektov, R. Yadav, M. Pizzochero, O. V. Yazyev, and M. A. McGuire, Applied Physics Letters **117** (2020).
[35] W. C. Jin, H. H. Kim, Z. P. Ye, S. W. Li, P. Rezaie, F. B. Diaz, S. Siddiq, E. Wauer, B. W. Yang, C. H. Li, S. J. Tian, K. Sun, H. C. Lei, A. W. Tsen, L. Y. Zhao, and R. He, Nature Communications **9** (2018).
[36] M. Kim, P. Kumaravadivel, J. Birkbeck, W. Kuang, S. G. Xu, D. G. Hopkinson, J. Knolle, P. A. McClarty, A. I. Berdyugin, M. Ben Shalom, R. V. Gorbachev, S. J. Haigh, S. Liu, J. H. Edgar, K. S. Novoselov, I. V. Grigorieva, and A. K. Geim, Nature Electronics **2,** 457 (2019).
[37] L. Ciorciaro, M. Kroner, K. Watanabe, T. Taniguchi, and A. Imamoglu, Physical Review Letters **124** (2020).
[38] M. C. Hessenbuettel, T. Deilmann, P. Krueger, and M. Rohlfing, Nano Letters **21,** 5173 (2021).
[39] J. K. Hu, J. X. Tan, D. Wu, Z. H. Zhang, and Z. Q. Fan, Applied Surface Science **560** (2021).
[40] Z. Yang, J. Wang, G. Hu, X. Yuan, J. Ren, and X. Zhao, Results in Physics **37** (2022).
[41] C. L. Tang, Z. W. Zhang, S. Lai, Q. H. Tan, and W. B. Gao, Advanced Materials **32** (2020).
[42] J. F. Dillon, Journal of Applied Physics **33,** 1191 (1962).
[43] C. S. Xu, J. S. Feng, H. J. Xiang, and L. Bellaiche, Npj Computational Materials **4** (2018).
[44] M. Farle, Reports on progress in physics **61,** 755 (1998).
[45] X. Yu, X. Zhang, Q. Shi, S. Tian, H. Lei, K. Xu, and H. Hosono, Frontiers of Physics **14,** 43501 (2019).
[46] S. Blundell, *Magnetism in Condensed Matter* (Oxford Univeristy Press Inc., New York, 2001).
[47] T. A. Tartaglia, J. N. Tang, J. L. Lado, F. Bahrami, M. Abramchuk, G. T. McCandless, M. C. Doyle, K. S. Burch, Y. Ran, J. L. Y. Chan, and F. Tafti, Science Advances **6** (2020).

[48] K. Kawasaki, Progress of Theoretical Physics **39,** 285 (1968).
[49] L. J. de Jongh, *Magnetic Properties of Layered Transition Metal Compounds* (Springer, Dordrecht, 1990).